

SPECTROSCOPIC AND MAGNETIC STUDIES OF ERBIUM DOPED
PHOSPHATE GLASS EMBEDDED WITH NATURAL FERRITE OXIDE
NANOPARTICLES

PUZI ANIGRAHAWATI

A thesis submitted in fulfilment of the
requirements for the award of the degree of
Master of Science (Physics)

Faculty of Science
Universiti Teknologi Malaysia

SEPTEMBER 2014

To my beloved father (H.Abu Bukhori) and my mother (Almh. Icah Napisah)

To my brothers and sisters (Denny, Robby, Fitri, Faiz and Tita)

for their enduring love, motivation and support

ACKNOWLEDGEMENTS

Alhamdulillah, thanks to Allah for giving me this opportunity, the strength and the patience to complete my thesis finally, after all the challenges and difficulties.

First and foremost, I would like to express my greatest gratitude to my supervisor Prof. Dr. Md. Rahim Sahar, who have guided and helped me a lot throughout my studies. I have been extremely lucky to have a supervisor who cared so much about my work, and who responded to my questions and queries so promptly. His advices on the morality and affability are certainly expensive lessons for me.

I am grateful to Mr. Mohd Jaafar bin Mohamad Jaafar Raji, Mr. Abdul Rahman bin Abdullah, Mrs. Nurhayah binti Jantan, Mrs. Radiyah binti Hassan, Mr. Yus Hamdan bin Yusof, Mr. Masrul bin Mansor, Mrs. Anisah binti Salikin, Sayidatul Hidayah binti Mhd. Nor for their cooperation in running the experiments for of this project.

Thanks to my supportive and friendship, Nurulhuda binti Mohammad Yusoff, Siti Amlah binti Mohammad Azmi, Ezza Syuhada binti Sazali, Khamisah binti Abu Samah, Asmahani binti Awang, Sharifah Fahsuhaizam binti Abd Rahman and other friends who were always supportive in my life and studies in this country.

My thanks also to Ministry of Education Malaysia for the MIS (Malaysia International Scholarship) award and financial support throughout this research study, which is really rewarding.

ABSTRACT

Erbium doped zinc phosphate glass embedded with natural Fe_3O_4 nanoparticles having a composition of $(69-x)\text{P}_2\text{O}_5 - 30\text{ZnO} - 1\text{Er}_2\text{O}_3 - (x)\text{Fe}_3\text{O}_4$, where $x = 0, 0.5, 1.0, 1.5, 2.0$ mol% has successfully been prepared by melt quenching technique. It was found that the color of the glass varies from pink (without natural Fe_3O_4 nanoparticles) to dark brown (2 mol% natural Fe_3O_4 nanoparticles). The change in color indicates that the natural Fe_3O_4 nanoparticles has already incorporated in the unit structure of the forming glasses. The amorphous structures of the glass sample were evident by the XRD analysis. The density and molar volume of the glass samples were found in the range of $2.75 - 2.89 \text{ g/cm}^3$ and $45.89 - 44.30 \text{ cm}^3$, respectively. The optical absorption edge was studied by using the UV-Vis spectroscopy. The optical band gaps for direct and indirect transitions and also Urbach energy varied in the range of $4.454 - 3.349 \text{ eV}$, $4.229 - 3.278 \text{ eV}$, and $0.637 - 0.233 \text{ eV}$, respectively were found to decrease with the increase of natural Fe_3O_4 nanoparticles contents. The emission spectrum was recorded using the photoluminescence spectrometer at room temperature. The emission spectra for 478 nm excitations displayed two prominent peaks centered at 532 nm and 634 nm that originate from $^4\text{S}_{3/2} \rightarrow ^4\text{I}_{15/2}$ and $^4\text{F}_{9/2} \rightarrow ^4\text{I}_{15/2}$ transitions, respectively. In addition, the intensity of luminescence spectra tends to quench the emission band with the increasing concentration of the natural Fe_3O_4 nanoparticles. The crystallite size of natural Fe_3O_4 nanoparticles was calculated using Debye-Scherrer formula and the results were compared with the size of nanoparticles obtained from TEM. The average diameter of the Fe_3O_4 nanoparticles of about 26 - 31 nm was calculated using Debye-Scherrer method and this value was about the same with that obtained by TEM micrographs. The TEM micrograph revealed the presence of spherical and homogenous distribution of natural Fe_3O_4 nanoparticles. Vibrating sample magnetometer (VSM) measurement showed that magnetization of glass increased with applied fields and showed paramagnetic and ferrimagnetic behavior.

ABSTRAK

Kaca zinc fosfat berdop erbium yang tersisip dengan nanopartikel Fe_3O_4 semulajadi dengan komposisi molar $(69-x)\text{P}_2\text{O}_5 - 30\text{ZnO} - 1\text{Er}_2\text{O}_3 - (x)\text{Fe}_3\text{O}_4$, dengan $x = 0, 0.5, 1.0, 1.5, 2.0$ mol% telah berjaya disediakan menggunakan teknik pelindapan leburan. Warna kaca didapati berubah daripada merah jambu (tanpa nanopartikel Fe_3O_4 semulajadi) ke coklat tua (2 mol% Fe_3O_4 semulajadi). Perubahan warna menunjukkan bahawa nanopartikel Fe_3O_4 semulajadi telah menyatu dalam struktur unit pembentukan kaca. Sifat amorfus sampel kaca telah disahkan oleh analisis XRD. Ketumpatan dan isipadu molar masing-masing adalah dalam julat $2.75 - 2.88 \text{ g/cm}^3$ dan $45.89 - 44.29 \text{ cm}^3$. Pinggir serapan optik dikaji menggunakan spektroskopi ultralembayung cahaya nampak. Jurang tenaga optik untuk peralihan terus dan tak terus serta tenaga Urbach masing-masing berada dalam julat antara $4.454 - 3.349 \text{ eV}$, $4.229 - 3.278 \text{ eV}$, dan $0.637 - 0.233 \text{ eV}$. Nilai ini didapati berkurang dengan pertambahan nanopartikel Fe_3O_4 semulajadi. Spektrum pancaran telah di rekod menggunakan spektrometer fotopendarcahaya pada suhu bilik. Spektrum pancaran diujakan pada 478 nm, menunjukkan kewujudan dua puncak yang berpusat di 532 nm dan 634 nm berasal dari transisi $^4\text{S}_{3/2} \rightarrow ^4\text{I}_{15/2}$ and $^4\text{F}_{9/2} \rightarrow ^4\text{I}_{15/2}$. Disamping itu, keamatan spektra pendarcahaya cenderung untuk mengurangkan jalur pancaran dengan pertambahan kandungan nanopartikel Fe_3O_4 semulajadi. Saiz hablur nanopartikel Fe_3O_4 semulajadi telah diperoleh menggunakan formula Debye-Scherrer dan dibandingkan dengan saiz nanopartikel yang diperoleh daripada mikroskop transmisi elektron (TEM). Nilai purata diameter nanopartikel Fe_3O_4 yang diperoleh ialah 26 – 31 nm dan nilai ini telah dikira menggunakan kaedah Debye-Scherrer didapati hampir sama dengan nilai yang dihasilkan oleh mikrograf TEM. Taburan mikrograf TEM menunjukkan kehadiran bentuk sfera dan taburan homogen nanopartikel Fe_3O_4 semulajadi. Pengukuran magnetometer sampel bergetar (VSM) menunjukkan bahawa pemagnetan kaca bertambah dengan medan yang dikenakan, serta menunjukkan perlakuan bahan paramagnetik dan ferimagnetik.

TABLE OF CONTENTS

CHAPTER	TITLE	PAGE
	DECLARATION	ii
	DEDICATION	iv
	ACKNOWLEDGEMENT	v
	ABSTRACT	vii
	ABSTRAK	viii
	TABLE OF CONTENTS	ix
	LIST OF TABLES	xii
	LIST OF FIGURES	xiii
	LIST OF ABBREVIATIONS	xvi
	LIST OF SYMBOLS	xviii
	LIST OF APPENDICES	xx
1	INTRODUCTION	
	1.1 Introduction	1
	1.2 Problem Statement	3
	1.3 Objectives of the Research	5
	1.4 Scope of Study	5
	1.5 Choice of System	6
2	LITERATURE REVIEW	
	2.1 Introduction	8
	2.2 Definition of Glass	8
	2.3 The Glass Formation	9
	2.4 Phosphate Glass Structure	11
	2.5 Rare Earth Ions	13

2.6	Fe ₃ O ₄ Nanoparticles	15
2.7	X-Ray Diffraction (XRD)	18
2.8	Physical Properties	20
2.8.1	Density and Molar Volume	20
2.9	Optical Properties	21
2.9.1	Absorption	21
2.9.2	Emission	22
2.9.3	Interband Absorption	22
2.9.4	UV-Vis-NIR Spectroscopy	25
2.10	Photoluminescence Spectroscopy (PL)	26
2.10.1	Light emission in solid	27
2.10.2	Interband Luminescence	29
2.11	Transmission Electron Microscopy (TEM)	31
2.12	Vibrating Sample Magnetometer (VSM)	32
2.13	Magnetism	33
2.13.1	Diamagnetism	33
2.13.2	Paramagnetism	34
2.13.3	Ferromagnetism	35
2.13.4	Ferromagnetic hysteresis	36

3

METHODOLOGY

3.1	Introduction	39
3.2	Raw Material	39
3.3	Power Mixing	40
3.4	Nominal Composition and Batch Calculation	40
3.5	Nanoparticles Preparation	41
3.6	Glass Preparation	41
3.7	X-Ray Diffraction (XRD)	43
3.8	Density Measurement	43
3.9	UV-Vis-NIR Spectroscopy	43
3.10	Photoluminescence Spectroscopy (PL)	44
3.11	Transmission Electron Microscopy (TEM)	44
3.12	Vibrating Sample Magnetometer (VSM)	45

4	RESULTS AND DISCUSSION	
4.1	Introduction	46
4.2	Glass Composition and Formation	46
4.3	Physical Properties	49
4.4	UV-Vis-NIR Spectroscopy	51
4.5	Luminescence Spectroscopy	56
4.6	Transmission Electron Microscopy (TEM)	59
4.7	Vibrating Sample Magnetometer (VSM)	61
5	CONCLUSIONS	
5.1	Introduction	68
5.2	Conclusion	68
5.3	Suggestion	70
	REFERENCES	71
	Appendix	78

LIST OF TABLES

TABLE NO.	TITLE	PAGE
1.1	The list of previous reseachers	4
3.1	A nominal compositions of P_2O_5 -ZnO- Er_2O_3 - Fe_3O_4 glass.	40
4.1	Nominal compositions of $(69-x)P_2O_5$ -30ZnO-1 Er_2O_3 - $(x)Fe_3O_4$ glass system.	47
4.2	Density and molar volume of the glasses system	49
4.3	The value of direct and indirect E_{opt} for the glass. The Urbach energy ΔE is also inserted.	53
4.4	The emission peaks of Er^{3+} in glass system	57
4.5	Experimental and calculated magnetic properties of the glasses.	64

LIST OF FIGURES

FIGURE NO.	TITLE	PAGE
2.1	The structural difference between (a) crystalline and (b) amorphous	9
2.2	Relation between glassy, liquid and crystalline solids	10
2.3	Energy level diagram for Er^{3+} ions	14
2.4	A section of the network of Fe_3O_4	15
2.5	(a) Face-centered cubic spinel structure of Fe_3O_4 (b) Magnification of one tetrahedron and one adjacent octrahedron sharing an oxygen atom	16
2.6	Inverse spinel structure of magnetite. The large spheres represent the oxygen atoms, the small dark spheres the site A and the small bright spheres denotes the B site.	17
2.7	Bragg's Law for the periodic arrangement atoms	18
2.8	Schematic XRD spectra in (a) crystal, (b) glass	19
2.9	Absorption process	21
2.10	The atomic emission	22
2.11	Interband optical absorption	23
2.12	Interband transition in solids: (a) direct band gap, (b) indirect band gap	25
2.13	A schematic diagram showing the light emitting in a solid	28
2.14	A schematic diagram of the interband luminescence process in a direct band gap material	30
2.15	A schematic diagram of the interband luminescence	31

	process in an indirect gap material	
2.16	Diamagnetic material; (a) without magnetic field, (b) magnetic field applied and (c) magnetic field removed	34
2.17	Paramagnetic material. (a) without magnetic field, (b) magnetic field applied and (c) magnetic field removed	35
2.18	Ferromagnetic material. (a) without magnetic field, (b) magnetic field applied and (c) magnetic field removed	36
2.19	Hysteresis curve of a ferromagnetic material	37
3.1	Glass preparation	42
4.1	Glass samples	48
4.2	A typical x-ray diffraction pattern of the glass	48
4.3	A typical x-ray diffraction pattern for PZEF5 glass	49
4.4	Density against the natural Fe ₃ O ₄ NPs content.	50
4.5	Molar volume against natural Fe ₃ O ₄ content	51
4.6	A plot of $(\alpha h\nu)^2$ against energy, $h\nu$	52
4.7	The plot of $(\alpha h\nu)^{1/2}$ against energy, $h\nu$	52
4.8	E_{opt}^D and E_{opt}^I vs natural Fe ₃ O ₄ (mol%) content	53
4.9	The Urbach energy of glasses versus natural Fe ₃ O ₄ concentration.	55
4.10	UV-Vis-NIR absorption spectra of the glass system	56
4.11	Luminescence spectra of Er ³⁺ doped zinc phosphate glasses with different natural Fe ₃ O ₄ concentration.	57
4.12	Schematic energy level diagram on Er ³⁺ ($\lambda_{ex}=478\text{nm}$)	58
4.13	Transmission electron microscopy image for PZEF4 glass	59
4.14	Histogram of the distribution of nanoparticles for PZEF4 glass	60
4.15	Transmission electron microscopy image for PZEF5 glass	60

4.16	Histogram of the distribution of nanoparticles for PZEF5 glass	61
4.17	Magnetization curve at room temperature of the natural Fe_3O_4 nanoparticles	62
4.18	Magnetization curves at room temperature for 0-2 mol% natural Fe_3O_4 nanoparticles doped glass	63
4.19	Magnetic susceptibility versus natural Fe_3O_4 concentration for the glass	64
4.20	NPs contents dependent variation remanent magnetization (M_r) of glasses.	65
4.21	Natural Fe_3O_4 concentration dependent Coercivity (H_c) of all samples.	66
4.22	Natural Fe_3O_4 concentration dependent Squarness (M_r/M_s) of all samples.	67

LIST OF ABBREVIATIONS

Al_2O_3	-	Alumunium Oxide
BO	-	Bridging Oxygen
DC	-	Down-Conversion
Er^{3+}	-	Erbium
ET	-	Energy Transfer
fcc	-	Face Centered Cubic
FeO	-	Wustite
Fe_3O_4	-	Ferrite Oxide or Magnetite
$\alpha\text{-Fe}_2\text{O}_3$	-	Hematite
$\gamma\text{-Fe}_2\text{O}_3$	-	Maghemite
FWHM	-	Full Length at Half Maximum
HR-	-	High-Resolution
HRTEM	-	High Resolution Transmission Electron Microscope
JCPDS	-	Joint Committee for Powder Diffraction Standards
JO	-	Judd-Ofelt
MgO	-	Magnesium Oxide
NBo		Non-Bridging Oxygen
NPs	-	Nanoparticle
NR	-	Non-Radiative
Oe	-	Oersted
P_2O_5	-	Phosphorus pentaoxide
P		Phosphorous atom
PL	-	Photo-Luminescence
RE	-	Rare Earth
TEM	-	Transmission Electron Microscope

UTM	-	Universiti Teknologi Malaysia
UV	-	Ultraviolet
VBM	-	Valence Band Maxima
VIS	-	Visible
VSM	-	Vibrating Sample Magnetometer
XRD	-	X-Ray Diffraction
ZnO	-	Zinc Oxide

LIST OF SYMBOLS

A	-	Absorption Coefficient
2θ	-	Angle of Diffraction
B	-	Magnetic Induction
d	-	Size of Nanoparticle, Thickness of the Sample
e	-	Charge of Electron
E	-	Electric Field
E_{dir}	-	Direct Optical Band Gap
E_{ind}	-	Indirect Optical Band Gap
$\Delta E, E_U$	-	Urbach Energy
f	-	Oscillator Strength
H	-	Magnetic Field
I	-	Intensity
l	-	Length
J	-	Orbit Angular Momentum
m	-	Mass of Electron
n_2	-	Non-linear Refractive Index
M	-	Average Molecular Weight
N	-	Concentration
N_A	-	Avogadro's number
R	-	Glass Constant
S	-	Stability Factor
T'	-	Transmission
T	-	Temperature
T_c	-	Crystallization Temperature
T_g	-	Glass Transition Temperature

T_m	-	Melting Temperature
T	-	Time
V	-	Molar Volume
W	-	Weight
α_m	-	Polarizability
β	-	Branching Ratio
E	-	Dielectric Function
X	-	Susceptibility
P	-	Density
λ	-	Wavelength
T	-	Lifetime
S	-	Spin
L	-	Orbit
ρ	-	Density
w_a	-	Weight of the glass sample in air
w_b	-	Weight of the glass sample in liquid
ρ_b	-	Density of Toluene
E_f	-	Energy of the final state
E_i	-	Energy of electron in lower band
B	-	Band tailing
$h\nu$	-	Photon energy
τ_R	-	Radiative lifetime
η_R	-	Luminescent efficiency
τ_{NR}	-	Non-radiative lifetime
M	-	Magnetic moment
H_c	-	Coercivity
M_r	-	Remanent magnetization
M_s	-	Saturation magnetization
M_r/M_s	-	Squarness

LIST OF APPENDICES

APPENDIX	TITLE	PAGE
A	The nominal composition of the glasses system	78
B	Calculation of apparent density and the error function	80
C	The direct band gap energy for each sample for the (69-x)P ₂ O ₅ -30ZnO-1Er ₂ O ₃ -(x)Fe ₃ O ₄ glasses system.	81
D	The indirect band gap energy for each sample for the (69-x)P ₂ O ₅ -30ZnO-1Er ₂ O ₃ -(x)Fe ₃ O ₄ glasses system.	83
E	The Urbach energy for each sample for the (69-x)P ₂ O ₅ -30ZnO-1Er ₂ O ₃ -(x)Fe ₃ O ₄ glasses system.	85
F	The emission spectra for each sample for the (69-x)P ₂ O ₅ -30ZnO-1Er ₂ O ₃ -(x)Fe ₃ O ₄ glasses system.	88
G	Electronic Balance Precisa 205 A SCS	90
H	Electrical furnace Model Thermolyne 47900	91
I	X-Ray Diffractometer	92
J	Precisa Model XT 220A	93
K	Schimaadzu UV-3101 PC scanning spectrophotometer	94
L	A Perkin Elmer LS-5S photoluminescence (PL) spectrophotometer	95
M	TEM Philips CM120	96
N	VSM Lake Shore 7400 series	97

CHAPTER 1

INTRODUCTION

1.1 Introduction

Glasses containing rare earth ions and embedded with magnetic nanoparticles (NPs) are getting large attention because the presence of NPs which may lead to the increase of luminescence intensity, thermal stability (Widanarto *et.al.*, 2013) and magnetic responsibility (Piaoping *et.al.*, 2009) (Hongxia *et.al.*, 2012). Among the current interest material, the P_2O_5 based glasses have attracted a large attention due to their various applications in optical data transmission, sensing and laser technologies. The characteristics of phosphate glasses include high transparency, low melting point, high thermal stability, and high gain density which is attributed to the high solubility of rare earth ions, low refractive index and low dispersion (Yung *et.al.*, 2011) (Das *et.al.*, 2009).

The choice of host glasses materials are very important in the development of optical devices doped with rare earth (RE). Among different glass host matrices, phosphate glasses have unique advantages over the other glass host matrices. Phosphate glasses matrices with suitable compositions have been found to be good hosts for different laser active ions (Talib *et.al.*, 2008). The properties of phosphate

glasses such as relatively high thermal expansion coefficients, low optical dispersions and low glass transition temperatures compare with their silicate or borate counterparts, make them technologically important material in spite of their hygroscopic and volatile properties. The hygroscopic behaviour of phosphate glasses and the volatility of P_2O_5 at elevated temperature are two of the main reason for the limited number of investigations on the structure and the properties of these glasses. However, due to all the good properties of phosphate glass, they are hygroscopic and the OH^- group which are present and acting like high energy phonons can severely affect the quantum efficiency of the emitting RE^{3+} . The main source of OH^- group is due to the starting material and the atmospheric moisture during the melting process hence there are some ways to reduce its incorporation in the glass by variations of composition and procedure (Andrea *et.al.*, 2008).

Glasses of the Er^{3+} have been reported to exhibit the largest magnetic contribution to the low temperature specific heats known in oxide glasses. Natural iron oxides, which are mostly in the form of magnetit (Fe_3O_4), hematite ($\alpha-Fe_2O_3$) and maghemite ($\gamma-Fe_2O_3$) can be easily found in iron sand. The $\alpha-Fe_2O_3$ has the same spinel structure as magnetite but has no divalent ions. The magnetic Fe^{3+} ions are positioned in two sublattices with different oxygen coordination. The ferrimagnetism arises from the unequal distribution of these ions in A and B sites. Recently, a low temperature spin glass transition was found at $T = 42$ K. The $\gamma-Fe_2O_3$ has a corundum crystal structure and has an antiferromagnetic order below 950 K, while above the Morin point (260 K) it exhibits so called weak ferromagnetism. Below melting temperature (T_m) the two magnetic sublattices are oriented along the rhombohedral [111] axis. The spin canting results in a weak ferromagnetic in the (111) plane. Hematite is the most stable iron oxide (Elena., 2004).

Incorporation of iron oxides into the glass has paramount importance due to their excellent magnetic, optical and electrical properties (Van., 1999). Magnetite (Fe_3O_4) is an important magnetic material that is widely used for different

applications such as magnetic sensors, printing ink and catalysts which especially in the biomedical field (Mazlini *et.al.*, 2012).

1.2 Problem Statement

The used of iron oxides (FeO , Fe_2O_3 and Fe_3O_4) as dopant has provide interesting phenomena over the structure and the properties of the phosphate glasses. In addition the iron-doped glasses exhibit interesting electrical and magnetic properties that depend on the iron oxide species and their coordination symmetry (Hussin, 2011). Fe_3O_4 nanoparticles are common ferrite oxides with an inverse spinal structure (Vijaya *et.al.*, 2005). These class of compounds exhibit unique electrical and magnetic properties due to the electron transfer between Fe^{2+} and Fe^{3+} in tetrahedral and octahedral sites. In addition, the transition metal ions will contribute to a multivalence state in the glass which influence the properties (Ensanya *et.al.*, 2009).

The effect of natural Fe_3O_4 nanoparticles (NPs) especially in the enhancement of emission intensity has been studied by few workers. Table 1.1 summerized the list of previous researchers regarding the studies on magnetic properties of glasses. However, there is a very limited study on the optical and magnetic properties of glass containing natural Fe_3O_4 NPs. Thus, it is the aim of this study to focus on both optical and magnetic properties in order to find their properties. It is expected that this study can provide more informations on the basic knowledge of the glass system.

Table 1.1 : The list of previous reseachers

Researcher	Title	Glass preparation technique	Material composition
Maximina Romero, <i>et. al.</i> , (2001)	Magnetic properties of glasses with high iron oxide content	Melt quenching technique	Fe ₂ O ₃ , SiO ₂ , Al ₂ O ₃ , CaO, MgO, ZnO, PbO, Na ₂ O, K ₂ O
I.S. Edelman, <i>et. al.</i> , (2001)	Superparamgnetic and ferrimagnetic nanoparticles in glass matrix	Melt quenching technique	Fe ₂ O ₃ , MnO, Li ₂ O, BaO
Mekki, <i>et.al.</i> , (2006)	Structural and magnetic investigation of Fe ₂ O ₃ -TeO ₂ glasses	Melt quenching technique	Fe ₂ O ₃ and TeO ₂
N.A. Zarifah, <i>et.al.</i> , (2010)	Magnetic behaviour of (Fe ₂ O ₃) _x (TeO ₂) _{1-x} glass system due to iron oxide	Melt quenching technique	Fe ₂ O ₃ and TeO ₂
J. Kaewkhao, <i>et.al.</i> , (2010)	Structural and magnetic properties of glass doped with iron oxide	Melt quenching technique	Na ₂ O, Al ₂ O ₃ , B ₂ O ₃ , CaO, Sb ₂ O ₃ , BaO, Fe ₂ O ₃
Ping Hu, <i>et.al.</i> , (2011)	Heat treatment on Fe ₃ O ₄ nanoparticles structure and magnetic properties prepared by carbothermal reduction	Carbothermal reduction method	Fe ₃ O ₄ , NH ₃ , H ₂ O
H. El. Ghandor	Synthesis and some physical propertis of magnetite (Fe ₃ O ₄) nanoparticles	Co-precipitation method	Fe ₃ O ₄ , NH ₄ , SO ₄ and FeCl ₃ .

1.3 Objectives of the Research

The objectives of the study are:

- i) To optimise the preparation of the Er^{3+} doped phosphate glasses of the $(69-x)\text{P}_2\text{O}_5-30\text{ZnO}-1\text{Er}_2\text{O}_3-(x)\text{Fe}_3\text{O}_4$ system ($x = 0, 0.5, 1.0, 1.5$ and 2.0 mol %).
- ii) To characterize the amorphous nature by using x-ray diffraction (XRD)
- iii) To determine the physical properties of the glass.
- iv) To characterize the glass by transmission electron microscope (TEM) imaging, UV-VIS and photoluminescence (PL) spectroscopy.
- v) To characterize the magnetic properties and the effect of nanoparticles.

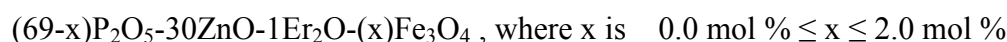
1.4 Scope of Study

In order to achieve the above objectives the works have been focused on the given scope :

- i. Ferrite oxide (Fe_3O_4) obtained from natural iron sand.
- ii. Preparation of glass based on the $(69-x)\text{P}_2\text{O}_5-30\text{ZnO}-1\text{Er}_2\text{O}_3-(x)\text{Fe}_3\text{O}_4$ system ($x = 0, 0.5, 1, 1.5$ and 2 mol %) using the melt quenching technique.
- iii. Characterization of amorphous nature by using XRD.
- iv. Determination of the density and molar volume of the glass system.
- v. Characterization of absorption by using UV-VIS-NIR spectrophotometer.
- vi. Characterization of emission by using Photoluminescence spectrophotometer.
- vii. Characterization of morphology of nanoparticles by using Transmission Electron Microscopy.
- viii. Characterization of magnetic properties by using Vibrating Sample Magnetometer.

1.5 Choice of System

To achieve the objectives of the study, a series of the glass system were chosen as below:



Phosphate glasses shows several advantages over conventional silicate and borate glasses due to their superior physical properties such as low melting and softening temperatures and high ultra-violet (UV) and far infrared transmission (Ensanya *et.al.*, 2009) (Khor *et.al.*, 2012). Important characteristics such as relatively high thermal expansion coefficients, low optical dispersions and low glass transition temperatures make them highly suitable for many applications. However, their very high hygroscopic nature due to excessive amount of OH^- contents limit the quantum efficiency of the emitting RE^{3+} ions which is decisive for device performance. The OH^- groups that mainly originates from the starting material and the atmospheric moisture during the melting process can considerably be reduced by incorporating suitable modifier such as ZnO and MgO in the host (Andrea *et.al.*, 2008) (Wiench *et.al.*, 2000).

There has been a continued interest among researcher in zinc phosphate glass system for various of application. The presence of zinc, which acting as a network former/modifier imparts better chemical durability, low glass transition temperatures and wider glass forming composition range. Due to higher transparency of zinc phosphate glasses in the ultraviolet region compared to conventional silicate glasses, UV light absorbing materials can be incorporated in these glasses (Dheeraj *et.al.*, 2009).

Iron oxide (Fe_3O_4) used as dopant provide interesting phenomena over structure and the properties of the phosphate glasses (Elisa *et.al.*, 2005). On the other hand, the iron-doped glasses exhibit interesting electrical and magnetic properties

due to the electron transfer between Fe^{2+} and Fe^{3+} in tetrahedral and octahedral sites. Here the electron Fe^{3+} moves to interface where it undergoes a one electron reduction to form electron Fe^{2+} . Furthermore, the transition metal ions will contribute multivalence state in the glass and dramatically influence the properties (Widanarto *et.al.*, 2013).

In recent times, glasses containing rare earth ions and embedded with magnetic nanoparticles are getting large attention because the presence of the NPs, which may lead to the increase of luminescence intensity, thermal stability and magnetic responsibility (Widanarto *et.al.*, 2013) (Piaoping *et.al.*, 2009) (Hongxia *et.al.*, 2012).

REFERENCES

- Aarts, L., Jaqx, S., Vander Eade, B.M., Meijerink, A. (2011). Down conversion for the Er^{3+} , Yb^{3+} couple in KPb_2Cl_5 - a low-phonon frequency host. *J. Luminescence*, 131 : 608-613
- Agarwal, A., Seth, V.P., Sanghi, S., Gahlot, P., Khasa, S. (2004). Mixed alkali effect in optical properties of lithium-potassium bismuth borate glass system. *J. Material Letters*, 58 : 694-698
- Andrea S S de Camargo., Idelma A A Terra., Luiz Antonio de O Nunes and M Siu Li. (2008). Energy transfer processes in Yb^{3+} - Tm^{3+} co-doped sodium alumino-phosphate glasses with improved 1.8 μm emission. *J. Phys.:Conds.Matt*, 20 : 255240
- Bhowmik R.N., Vasanthi V., Asok Poddar. (2013). Alloying of Fe_3O_4 and Co_3O_4 to develop $\text{Co}_{3x}\text{Fe}_{3(1-x)}\text{O}_4$ ferrite with high magnetic squareness, tunable ferromagnetic parameters, and exchange bias. *J. Alloys. Compd*, 578 : 585-594
- Bingham, P.A., Hand, R.J., Hannant, O.M., Forder, S.S., Kilcoyne, S.H. (2009). Effect of modifier additions on the thermal properties, chemical durability, oxidation state and structure of iron phosphate glasses. *J. Non-Cryst. Solids*, 355 : 1526-1538
- Bubb. R. Cupertino. (1999). Basic of X-Ray Diffraction . Scintag. Inc. USA
- Chanshetti, U.B., Shelke, V.A., Jadhav, S.M., Shankarwr, S.G. (2011). Density and volume studies of phosphate glasses. *J. Physics, Chemistry and Technology*, 9 : 29-36

- Che-Zoue Weng., Jia-Hong Chen., Ping-Yu Shih. (2009). Effect of dehydroxylation on the structure and properties of $\text{ZnCl}_2\text{-ZnO-P}_2\text{O}_5$ glasses. *J. Mater. Chem. Phys*, 115 : 628-631
- Das, S.S., Singh, N.P., Srivastava, P.K. (2009). Ion conducting phosphate glassy materials. *J. Crystall Growth and Characterization of Materials*, 55 : 47-62
- David B., Willams and Barry Carter, C. (1996). Transmission Electron Microscopy, Plenum Press New York, USA, p.5
- Dheeraj Jain., Sudarsan, V., Vatsa, R.K., Pillai, C.G.S. (2009). Luminescence studies on $\text{ZnO-P}_2\text{O}_5$ glasses doped with $\text{Gd}_2\text{O}_3\text{:Eu}$ nanoparticles and Eu_2O_3 . *J. Lumin*, 129 : 439-443
- Elena-Lorena Salabas, Horezu-Rumanien. (2004). Structural and Magnetic Investigations of Magnetic Nanoparticles and Core Shell Colloids. Tag Der Mundlichen Prufung
- Elisa, M., Cristiana, E.A., Grigovescu. (2005). Optical and electronic properties of the aluminophosphate glasses doped with 3D-transition metal ions. *J. Matter Science*, 10 : 367-374
- Ensanya, A., Abou Neel., Chrzanowski., Wojciech., Pickup., David M., O'Dell, L.A., Mordan., Nicola, J., Newport., Robert, J., Smith., Mark, E., Knowles., Jonathan C. (2009). Structure and properties of strontium-doped phosphate-based glasses. *Journal of The Royal Society Interface*, 6 : 435-446
- Fox, M. (2010). Optical Properties of Solids. New York : Oxford University Press
- Foner, S. (1959). Versatile and sensitive vibrating-sample magnetometer, *J. Review of Scientific Instruments*, 30 : 548
- Ghandor, El.H., Zidan, H.m., Mostafa, M.H., Khalil., Ismail, M.I.M. (2012). Synthesis and some physical properties of magnetic (Fe_3O_4) nanoparticles. *J.Elect. Sci*, 7 : 5734-5745

- Harris, I.R., Williams, A.J. (1994). Magnetic Materials. *Material Science and Engineering* Vol II, Birmingham, UK
- Hongxia Peng., Bin Cui., Leilei Li., Yingsai Wang. (2012). A simple approach for the synthesis of bifunctional $\text{Fe}_3\text{O}_4@\text{Gd}_2\text{O}_3:\text{Eu}^{3+}$ core-shell nanocomposite. *J. Alloys. Compds*, 531 : 30-33
- Hooi M.O., Halimah M.K., Wan M.D.W.Y. (2012). Optical Properties of Bismuth Tellurite Based Glass. *International Journal of Molecular Science*. 13: 4623-2631.
- Hu P.H.B., Yang, D.A. Pan, J.J. Tian, S.G. Zhang, A.A Volinsky, (2010). Carbothermal reduction method for Fe_3O_4 powder syhthesis. *J. Alloys. Compd*, 502 : 338-340
- Hussin Rosli. (2011). Structural Studies of Glass by Nuclear Magnetic Resonance: UTM Press, UTM
- Kaliski.Y, Reisfeld,R.Haas.Y. (1979). *J. Chem.Phys.Lett*. 61 : 19-22.
- Khor, S.F., Thalib, Z.A., Mat Yunus, W.M. (2012). Optical properties of ternary zinc magnesium phosphate glasses. *J. Cer. Inter*, 38 : 935- 940
- Kranjc̃ec, M., Studenyak, I.P., Kurik, M.V. (2009). On the Urbach rule in non-crystalline solids. *Journal of Non-Crystalline Solids*, 355 : 54–57
- Licina, V., Mogus, A., Milankovic., Reis, S.T., Dax, D.E. (2007). Electronic conductivity in zinc iron phosphate glasses. *J. Non-Cryst. Solids* 353 : 4395-4399
- Lin, H., Liu, K., Pun, Y.B., Ma, T.C., Peng, X., An, Q.D., Yu, J.Y., Jiang, S.B. (2004). Infrared and visible flourescence in Er^{3+} -doped gallium tellurite glasses. *J. Chem.Phys.Lett*. 398 : 146-150
- Liying Zhang, Yafei Zhang, (2009). Fabrication and magnetic properties of Fe_3O_4 nanowire arrays in different diameters. *J. Mag. Mag. Matt*, 321 : L15-L20

- Martin Friak, Arno Schindlmayr, Matthias Scheffler. (2007). An initio study of the half-metal to metal transition in strained magnetite. *New Journal of Physics*. 9 : 5
- Maximina Romero., Jesus Ma., Rincon., Carlos J. R. Gonzalez Oliver., Carlos D'Ovidio., Daniel Esparza., (2001). Magnetic properties of glasses with high iron oxide content. *J. Materials Research Bulletin*. 36 : 1513-1520
- Mazlini Mazlan., Sahar, M.R., Ariffin, R., Rohani, M.S. (2011). Optical absorption of $\text{Er}^{3+}/\text{Nd}^{3+}$ co-doped magnesium phosphate glass. UMTAS
- Nandyala Sooraj. H., Jose Domingos D. S. S . (2008). Physics and chemistry of Rare-Earth ions doped glasses. *J. Trans Tech Publication*. Switzerland.
- Niyafar, M., Ahmadi, A., Hasanpour, A. (2012). Synthesis of zinc ferrite nanoparticles. *J. World Applied Science* 17 : 739-741
- Noorsyam.Y. (2008). Optical and thermal properties of samarium oxide doped tellurite glass. Universiti Teknologi Malaysia: M.Sc Thesis
- Nurulhuda, M.Y. (2011). Optical properties of magnesium phosphate glass doped samarium. University Teknologi Malaysia: M.Sc Thesis
- Obaid ur Rahman., Subash Chandra Mohapatra., Sharif Ahmad. (2012). Fe_3O_4 inverse spinal super paramagnetic nanoparticles. *Journal of Materials Chemistry and Physics*, 132 : 196-202
- Piaoping Yang., Zewei Quan., Zhiyao Hou., Chunxia Li., Xiaojiao Kang., Ziyong Cheng., Jun Lin. (2009). A magnetic, luminescent and mesoporous core-shell structured composite material as drug carrier. *J. Biomaterials* 30 : 4786 - 4795
- Ping Hu., Shengen Zhang., Hua Wang., De'an Pan., Jianjun Tian., Zhi tang., Alex A. Volinsky. (2011). Heat treatment effects on Fe_3O_4 nanoparticles structure and magnetic properties prepared by carbothermal reduction. *J. Alloys. Compd*, 509 : 2316-2319

- Porthun, S., Abelman, L., Lodder, C. (1998). Magnetic force microscopy of thin film media for high density magnetic recording. *J. Magn. Magn. Mat*, 182 : 238
- Prithviraj Swamy, P.M., Basavaraja, S., Arunkumar Lagashetty., Srinivas Rao, N.V., Nijagunappa, R., Venkataraman, A. (2011). Synthesis and characterization of zinc ferrite nanoparticles obtained by self-propagating low-temperature combustion method. *J. Mater. Sci*, 34 : 1325–1330
- Raja Amjad, J., Sahar, M.R., Ghosal, S.K., Dousti, M.R., Riaz, S., Tahir., B.A. (2012). Optical investigation of Sm^{3+} doped zinc-lead-phosphate glass. *J. Phys. Lett*, 29 : 087304
- Rani, S., Sanghi, S., Agarwal, A., Ahlawat, N. (2009). Influence of Bi_2O_3 on optical properties and structure of bismuth lithium phosphate glasses. *J. Alloys. Compd*, 477 : 504-509
- Reis, S.T., Karabulut, M., Day, D.E. (2001). Chemical durability and structure of zinc-iron phosphate glasses. *J. Non-Cryst. Solids*, 292 : 150-157
- Reza Dousti, M., M.R. Sahar, S.K Ghoshal, Raja J., R. Arifin. (2013). Plasmonic enhanced luminescence in Er^{3+} : Ag co-doped tellurite glass. *J. Mol. Strc*, 1033 : 79-83
- Scintag. (1999). Basics of X-Ray Diffraction. Bubb Road Cupertino. U.S.A
- Sharaf El-Deen, L.F., Al Salhi, M.S., Meawad, M., Elkholy. (2008). IR and UV spectral studies for rare earth-doped tellurite glasses. *J. Alloys. Compds*, 465 : 333–339
- Shih, P.Y. (2004). Thermal, chemical and structural characteristics of erbium-doped sodium phosphate glasses. *J. Chemistry and Physics*, 84 : 151-156
- Sidek H.A.A., Rosmawati S., Talib Z.A., Halimah M.K., Daud W.M. (2009). Synthesis and Optical Properties of $\text{ZnO} - \text{TeO}_2$ Glass System. *American Journal of Applied Sciences*. 6(8): 1489 – 1494.

- Sulhadi. (2007). Structural and optical properties studies of erbium doped tellurite glasses. Universiti Teknologi Malaysia : Ph. D. Thesis
- Talib, Z.A., Daud, W.M., Tarmizi, E.Z.M., Sidek, H.A.A., Yunus, W.M.M. (2008). Optical absorption spectrum of $\text{Cu}_2\text{O-CaO-P}_2\text{O}_5$ glasses. *J. Physics and Chemistry of Solids*, 69 : 1969-1973
- Van Deun, R., K. Binnemans, C. Gorller-Walrand., J.L. Adam. (1999). Spectroscopic properties of trivalent samarium ions in glasses. *SPIE conference on Rare-Earth doped materials and devices III.*, Vol 3622
- Vemula Venkatramu., Sergio F. Leon-Luis., Ulises R. Rodriguez-Mendoza., Virginia Monteseguro., Francisco J. Manjon., Antonio D. Lozano-Gorrin., Rafael Valiente., Daniel Navarro-Urrios., Jayasankar Alfonso Muno, C.K., Victor Lavin. (2012). Synthesis, structure and luminescence of Er^{3+} doped $\text{Y}_3\text{Ga}_5\text{O}_{12}$ nano-garnets. *J. Materials Chemistry*, 22 : 13788
- Vijaya, M.S., Rangarajan, G.J. (2005). Materials Science. Delhi: Tata McGraw-Hill
- Widanarto, W., Sahar, M.R., Ghoshal, S.K., Arifin, R., Rohani, M.S., Effendi, M. (2013). Natural Fe_3O_4 nanoparticles embedded zinc-tellurite glasses: polarizability and optical properties. *J. Materials Letters*, 108 : 289-292
- Widanarto, W., Sahar, M.R., Ghoshal, S.K., Arifin, R., Rohani, M.S., Hamzah, K. (2013). Effect of natural Fe_3O_4 nanoparticles on structural and optical properties of Er^{3+} doped tellurite glass. *J. Magnetism and Magnetic Materials*, 326 : 123-128
- Wiench, J.W., Pruski, M., Tischendorf, B., Otaigbe, J.U., Sales, B.C. (2000). Structural studies of zinc polyphosphate glasses by nuclear magnetic resonance. *J. Non-Cryst. Solids*, 26 : 101-110
- Wiley-Vch Verlag GmbH., Co kGaA. (2007). Magnetic Nanoparticles. Russian Academy of Science : Moscow

- Xiao Juan Liang., Haowei Shi., Xiang Chen Jia., Yuxiang Yang., Xiangnong Liu. (2011). Dispersibility, shape and magnetic properties of nano-Fe₃O₄ particles. *J. Materials Sciences and Application*, 2 : 1644-1653
- Yu. S. Dedkov, M.Fonin, D. V. Vyalikh, J. O. Hauch, S. L. Molodtsov, U. Rudiger, G. Guntherodt. (2004). Electronic structure at the Fe₃O₄ (111) surface. *Journal of Physical Review B*. 70 : 073405
- Yung, S.W., Hsu, S.M., Chang, C.C., Hsu, K.L., Chin, T.S., Hsiang, H.I., Lai, Y.S. (2011). Thermal, chemical, optical properties and structure of Er³⁺-doped and Er³⁺/Yb³⁺-codoped P₂O₅-Al₂O₃-ZnO glasses. *J.Non-Cryst. Solid*, 357 : 1328–1334
- Zarifah, N.A., Halimah, M.K., Hashim, M., Azmi, B.Z., Daud, W.M. (2010). Magnetic behaviour of (Fe₂O₃)_x(TeO₂)_{1-x} glass system due to iron oxide. *J. Chalcogenide letters*, 7 : 565-571
- Zheng tao, Qin Jie-Ming, Jiang Da-Yong, Lu Jing wen, Xiao Sheng-Chum. (2012). Spectroscopic properties in Er³⁺/Yb³⁺ co doped fluorophosphate glass. *J. Chin.Phys.B*. 20 : 043302